Radiography for a Shock-accelerated Liquid Layer

P. Meekunnasombat[1], **J.G. Oakley**[2], **M.H. Anderson**[2], **and R. Bonazza**[2]

[1] *Institut de Radioprotection et de Sûreté Nucléaire (IRSN), Centre de Cadarache, Saint Paul Lez Durance, France*
[2] *Department of Engineering Physics, University of Wisconsin-Madison, Madison, WI, USA*

Abstract. A flash X-ray radiography technique is employed to measure the volume fraction of a shock accelerated liquid layer in a large vertical shock tube. A series of the fragmented liquid layer X-ray snap-shots are taken at different post-shock times and pieced together to reconstruct the entire volume fraction field of the shock-induced breakup at Mach 2.12. A rapid development of the gas-liquid mixing layer is found as water layer that is initially 12.8 mm thick spreads to 22.5 cm in 3.2 ms.

1   Introduction

A quantitative measurement of the fragmentation of a liquid layer subjected to a shock wave is important to understand how a liquid sheet absorbs a blast wave. One application of this shock absorption concept is for an inertial fusion energy (IFE) reactor. An IFE reaction produces a shock wave that emanates from the center of the reactor chamber to the first wall. One proposed idea is to use liquid sheets/jets of molten salt to protect the first wall from fusion debris and absorb thermal energy. Water has been widely used to study the dynamics of the molten salt experimentally [1–3] because it is much easier to handle and can be scaled [4,3] to the molten salt.

A flash X-ray technique was used to measure the shock-induced mixing of a gas interface by Bonazza and Sturtevant [5,6] to study the Richtmyer-Meshkov instability. The work successfully accomplished quantitative densitometry and useful data was extracted from the X-ray negatives. In the present work, a similar X-ray radiography technique is employed to quantify the volume fraction of a shocked water layer with the aid of more modern imaging instrumentation. Rather than measuring X-ray radiation directly using sophisticated nuclear instruments [7], the strength of the X-ray absorption is measured and calibrated from the density of the X-ray image on a conversion screen.

2   Experimental Setup

Experiments are conducted in a 9.2 m long vertical shock tube with a square internal cross-section, 25.4 cm sides [8]. The flat water layer is supported in a square frame (same dimensions as the cross-section of the shock tube) with a 0.94 μm thick Mylar (polyethylene terephthalate) film and 19 nylon wires (0.3 mm diameter) spanning the width of the frame (12.7 mm apart, initial tension on a nylon wire is approximately 10.5 N) beneath the film to minimize sag. The driven section (0.455 m^3) is evacuated and filled to atmospheric pressure with argon (twice) to achieve a gas purity greater than 99%. The frame containing the water layer is then placed in the shock tube interface section located 46.4 cm above the centerline of the imaging window in the test section as shown in Fig. 1.

The driver section (0.364 m^3, not shown) is above the driven section, and separated from it by a metal diaphragm; the driver is pressurized, with either helium or nitrogen depending on the desired shock strength, to within 5% of the rupture pressure of the diaphragm. A boost tank (0.054 m^3, not shown), connected to the driver section through a fast acting valve, is pressurized to about 20% more than the diaphragm rupture pressure. The experiment begins when the fast acting valve from the boost tank to the driver section is opened and the high pressure gas in the boost tank over-pressurizes the driver to rupture the diaphragm. The high pressure in the driver pushes the diaphragm to cut along a cross-shaped knife edge beneath it to maintain a consistent rupture pressure. A planar shock wave propagates down from the diaphragm section to the interface section. Piezoelectric pressure transducers are flush-mounted along the inside wall and in the end-wall of the shock tube to measure the dynamic pressures inside the tube. One of these pressure transducers (above the interface section) is used as a trigger for the data acquisition (DAQ) unit which records these pressure data and to trigger an X-ray pulse for imaging inside the test section.
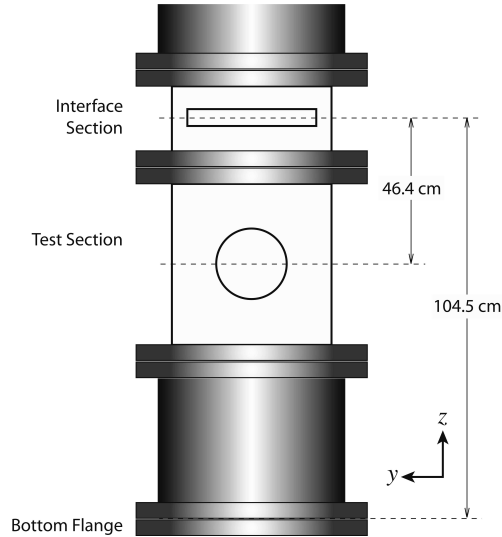
Fig. 1. Schematic of the lower portion of the shock tube.

Radiography has a significant advantage over either shadowgraph or planar imaging techniques [9] in that it can provide quantitative data about the shocked water layer. Since the X-rays that traverse different water depths are recorded as different gray scales, the mass fraction of the shocked water layer can be deduced.

A schematic of the X-ray system setup is shown in Fig. 2. A flash X-ray source (Hewlett-Packard Flash X-Ray Electron Beam system, model 43731A) is mounted 15.2 cm from the front window of the test section. The source generates a 70 ns X-ray flash, with a maximum photon energy of 150 KeV, and is aligned with the test section windows (12.7 cm diameter, 0.635 cm thick, T300 grade carbon fiber composite: used in aerospace applications and chosen because of their relative transparency to X-rays) and projects onto a conversion screen (Kodak Lanex fast screen: used in medical diagnostics) on the

other side of the test section. The operation begins with supplying an appropriate pressure of N_2 (172 kPa) into the pulser unit and then the high voltage supply is gradually increased to about 30 kV. A trigger signal, supplied either manually or from the DAQ, causes the pulser to send a high voltage pulse to the X-ray tube (model 130-529500) causing a large electron flux from the cathode. As the electrons impact on the anode at high velocity a pulse of X-rays is emitted. The conversion screen is mounted on a flat board inside a light-proof box (Fig. 2). The screen generates a fluorescent flash of green light on the back when stimulated by the X-ray photons. The 16-bit, 1024×1024 pixel array CCD camera (PixelVision Inc.'s SpectraVideo camera, model SV10kV1B/IYT-W3) inside the box is focused on the screen (using a Nikkor 50 mm f/1.2 lens with 8 mm extension tube, Nikon PK-11A). The camera shutter is opened approximately 1-2 seconds before the X-ray flash and closed 2-3 seconds later.
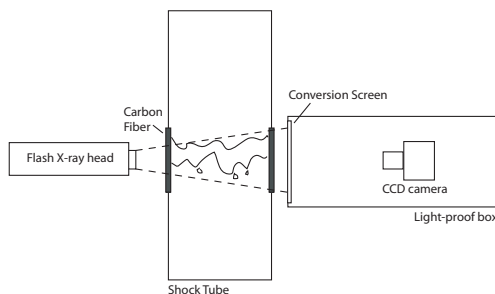

Fig. 2. Side view of the X-ray system with the shock tube and CCD camera.

3   Results

Figure 3A is a raw X-ray image signal (I_S) of a shocked water layer. The water depth (x_w, line of sight) is determined using:

$$x_w = \frac{1}{\mu_{Ar,hp} - \mu_w} \ln \left[\left(\frac{I_S - I_D}{I_{bg} - I_D} \right) e^{(\mu_{Ar,hp} - \mu_{Ar})x_{st}} \right], \tag{1}$$

where μ is an experimentally determined attenuation coefficient [10] for water, argon, or high pressure argon; I_D is the noise signal (dark current, readout, gain, etc.); I_{bg} is a background signal of the argon acquired before the test; and x_{st} is the depth of the test section, 25.4 cm. The average attenuation coefficient obtained for the water is μ_w=0.1714 cm^{-1} which corresponds to that obtained from a standards measurement with a 99 keV photon source [11]. Figure 3B shows percent volume fraction (x_w/x_{st}) of the water in the test section. The lighter areas indicate a higher volume fraction of water.

The left hand side of Fig. 4 are the 2-D grayscale maps of water volume fraction of a shocked water layer (initially 12.8 mm thick), and the right hand side are the average volume fractions, for each row, along the vertical position within the region of interest (rectangle shown in Fig. reffig:test160B). The series are shown in a *reverse chronological* order from the top to visualize the shocked water layer that is moving downward. The leading edge of the shocked water layer is imaged and shown in the bottom image of
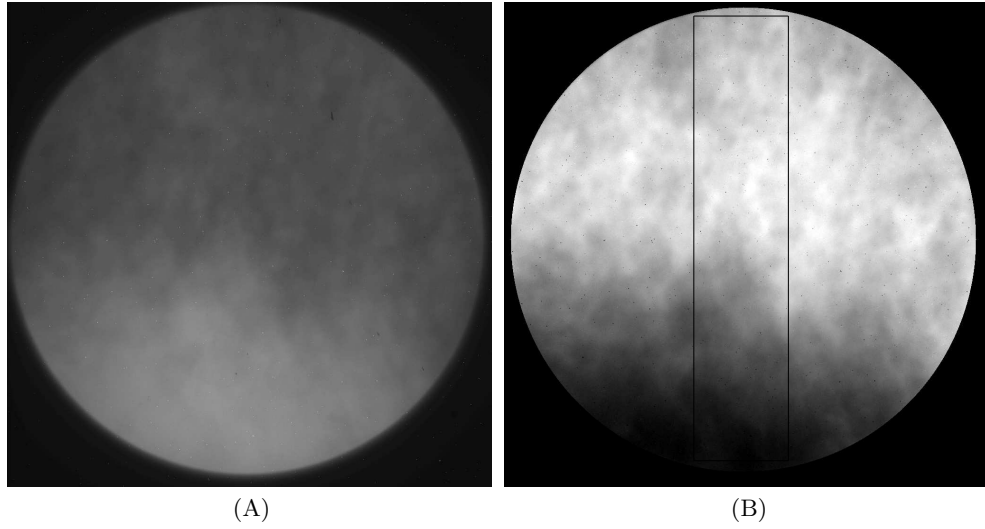
Fig. 3. (A) X-ray image of an initially 12.8 mm thick water layer 3.19 ms after contact by $M=2.12$ shock wave, (B) converted to percent water volume fraction.
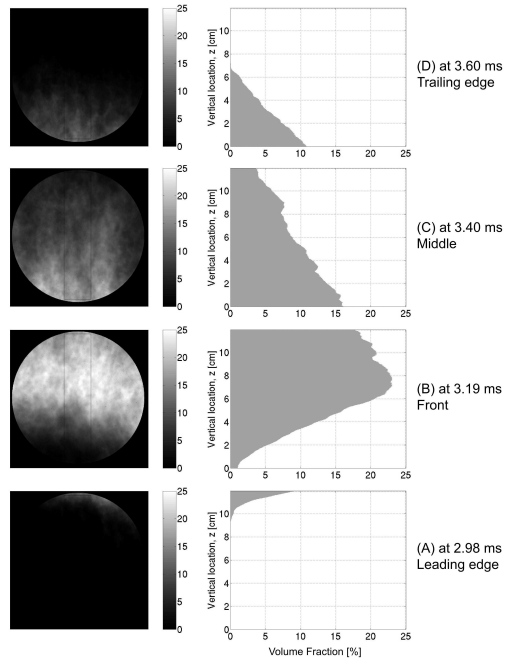

Fig. 4. An initially 12.8 mm thick water layer subjected to a $M=2.12$ shock wave.

Fig. 4 taken 2.98 ms after the initial shock-layer contact. The main body of the water is seen in the second and third images from the bottom (Figs. 4B and C), taken at 3.19 ms and 3.40 ms, respectively. The image at the top (Fig. 4D) shows the trailing edge of the shocked water layer imaged 3.60 ms after the contact. These plots are then combined, and with the aid of the overlapping areas, yield a volume fraction plot of the entire span of the shocked water layer as shown in Fig. 5. The volume fraction of water approaches a peak of 22.5% at a faster rate than the following decrease. The result shows that an initially flat water layer (12.8 mm thick) is stretched to about 18 times its original thickness (from the beginning of the leading edge to the end of the trailing edge) by a $M=2.12$ shock wave within 3.2 ms, with an average volume fraction of 11.5%.
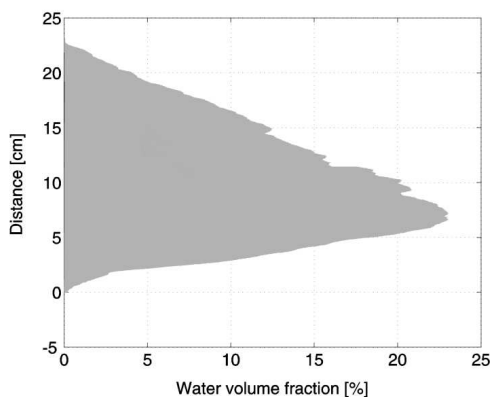

Fig. 5. Percent volume fraction of an initially 12.8 mm thick water layer, approximately 3.2 ms after being accelerated by a $M=2.12$ shock wave.

4   Conclusion

Flash X-ray radiography enables quantitative measurement of the shocked water layer volume fraction in a shock tube. The measurements show that the impact of the shock wave with the liquid layer is drastically different from simply convecting the layer downstream with the particle velocity; a large amount of energy has gone into breaking-up the liquid and generating a broad two-phase flow regime. It is found that the shock-induced spread of an initially 12.8 mm thick liquid layer develops very rapidly– to 18 times its original thickness within 3.2 ms at $M=2.12$ with a maximum volume fraction of 22.5%. The spread near the leading edge of the shocked layer is less than that near the trailing edge behind it.

There are three major factors that effect the uncertainty of the measurement namely: the diverging characteristic of the beam that distort the projection image; the non-linear response of the conversion screen; and the screen bleeding. The image distortion due to the diverging beam will become minimal in a smaller tested area as the beam appears to be more collimated. An appropriate X-ray energy can be used with a certain size of the test section and the test medium to minimize the uncertainty. An optimum X-ray energy for a certain test section size that gives a minimum uncertainty is presented by

Kendoush and Sarkis (2002) [7]. However, this technique can be applied in other shock tubes and high-speed flow experiments to visualize the flow density within a prescribed accuracy.

Acknowledgement

References

1. L.C. Elwell, D.L. Sadawski et al.: 'Dynamics of oscillating turbulent liquid sheets,' Fusion Tech. **39** n.2,2 pp 716–720 (2001)
2. R. Abbott, S. Pemberton, P.F. Peterson, G.P Sun, P. Wright, R. Holmes, J. Latkowski, R. Moir, K. Springer: 'Cylindrical liquid jet grids for beam-port protection of thick-liquid heavy-ion fusion target chambers,' Fusion Tech. **39** n.2,2 pp 732–738 (2001)
3. S.J. Pemberton: Thick Liquid Protection in Inertial Fusion Power Plants. Ph.D. Thesis, University of California-Berkeley (2002)
4. C. Jantzen, P.F. Peterson: 'Scaled impulse loading for liquid hydraulic response in IFE thick-liquid chamber experiments,' Nuclear Instr. & Meth. in Phys. Res A **464** pp 404–409 (2001)
5. R. Bonazza, B. Sturtevant: 'X-ray measurements of shock-induced mixing at an Air/Xenon interface,' *Proc. 4th Intl. Workshop on the Phys. of Compressible Turbulent Mixing, Cambridge* pp 194–200 (1993)
6. R. Bonazza, B. Sturtevant: 'X-ray measurements of growth rates at a gas interface accelerated by shock waves,' Phys. Fluids **8**(9) pp 2496–2512 (1996)
7. A.A. Kendoush, Z.A. Sarkis: 'Void fraction measurement by X-ray absorption,' Expm. Ther. & Fluid Sci. **25** pp 615–621 (2002)
8. M.H. Anderson, B.P. Puranik, J.G. Oakley, P.W. Brooks, R. Bonazza: 'Shock tube investigation of hydrodynamic issues related to inertial confinement fusion,' Shock Waves **10**(5) pp 377–387 (2000)
9. P. Meekunnasombat, J.G. Oakley, M.H. Anderson, R. Bonazza: 'Experimental study of a shock-accelerated liquid layer.' *24th Intl. Symp. on Shock Waves Proc., Beijing China, Paper 2692* (2004)
10. P. Meekunnasombat: Experimental Study of Shock-accelerated Liquid Layers for Protection of Inertial Fusion Energy Reactors. Ph.D. Thesis, University of Wisconsin-Madison (2004)
11. J.H. Hubbell, S.M. Seltzer: 'Table of X-ray Mass Attenuation Coefficients and Mass Energy-Absorption Coefficients (version 1.4),' Natl. Inst. of Std. and Tech., Gaithersburg MD, *[Online] http://physics.nist.gov/xaamdi* (2004)